Interaction of a tunable probe beam with a high-intensity pulsed CO_2-laser beam in p-type germanium

R. B. James
Solid State Division, Oak Ridge National Laboratory, Oak Ridge, Tennessee 37831

D. L. Smith*
California Institute of Technology, Pasadena, California 91125
(Received 5 August 1983)

A theoretical study is presented of the interaction between a high-intensity pump beam with a wavelength of 10.6 μm and a low-intensity probe beam which is tunable in the (9—11)-μm region. The dominant absorption mechanism of the optical beams in p-type Ge is direct intervalence-band transitions between states in the heavy- and light-hole bands. The hole states in resonance with the pump tend to saturate at sufficiently high intensities due to changes in the occupation probabilities of the initial and final states. When the material is simultaneously irradiated by the pump and probe beams, there is a nonlinear response which produces a component in the hole population difference between the heavy- and light-hole bands which oscillates at the beat frequency. This oscillating component in the population difference acts as a spatial and temporal grating which mixes the two beams. The absorption of the probe beam is modified by the presence of the pump beam by both the saturation of the intervalence-band transitions and by the oscillating population difference, which can scatter pump photons into the direction of the probe beam with the frequency shifted to that of the probe. Calculations of the probe absorption as a function of the frequency difference between the probe and pump beams are presented. These calculations of the absorption spectrum are compared with experimental results and good agreement is found. In addition to modifying the probe absorption spectrum, the oscillating population difference leads to a current-density component which oscillates at the pump frequency plus the beat frequency. If the pump and probe beams are nearly phase matched, this current-density component can generate a new optical beam that oscillates at the pump frequency plus the beat frequency. The intensity of this generated wave is estimated as a function of the beat frequency and the pump and probe intensities.

I. INTRODUCTION

In many p-type semiconductors, the absorption of light with photon energies less than the band gap is dominated by direct free-hole transitions. For light in the CO_2-laser spectrum ($\lambda \sim 10$ μm), these intervalence-band transitions in p-type GE occur between the heavy- and light-hole bands, whereby a free hole in the heavy-hole band absorbs a photon and makes a direct transition to a state in the light-hole band.[1] The absorption due to the intervalence-band transitions in p-type Ge has been experimentally shown to saturate at high CO_2-laser intensities in a manner closely approximated by an inhomogeneously broadened two-level model.[2–6] Theoretical calculations suggested that this nonlinear behavior of the absorption coefficient results from a population effect in which the hole-occupation probabilities for states in the resonant region of the heavy- and light-hole bands begin to approach one another at high light intensities.[4,7–10]

Experimental attempts have been made to understand the response of the free-hole distribution to a high-intensity pump of fixed wavelength by measuring the transmission of a weak tunable probe also resonant between the heavy- and light-hole bands.[4,11,12] By measuring the transmission of the probe beam as a function of the detuning of the pump and probe, one can investigate the modification of the free-hole distribution by the high-intensity pump for states nearly resonant with the pump laser. The specific features of the spectral linewidths of the probe absorption also yield valuable information on the relaxation times.

In this paper, we present calculations of the absorption line shape of the probe beam as a function of the intensity of the pump beam. The absorption coefficient of the probe beam is found to consist of two separate contributions. One part is due to the decrease in the distribution of free holes in the resonant region of the heavy-hole band induced by the saturating beam. The hole-burning effect can be described using the theory presented in Ref. 13, in which rate equations are constructed to determine the distribution of hole states in $\vec{k}$ space as a function of the intensity of the saturating beam. The second part results from the nonlinear response of the hole distribution to a forcing oscillation at the beat frequency Δ ($\Delta=\omega_+-\omega_-$) for a pump laser with frequency ω_+ and a probe laser with frequency ω_-. This forcing oscillation induces pulsations of the difference in occupation probabilities between states in the resonant region of the heavy- and light-hole bands. These population pulsations act as a temporal and spatial laser-induced grating which can scatter pump photons into the direction of the probe beam with the frequency shifted to that of the probe beam, and

vice versa. This coherent scattering can have a significant influence on the light transmission as measured in the probe direction. The calculated results show that the light as measured along the probe direction cannot be directly related to the response of the semiconductor due to the presence of the pump beam alone. The contribution from the coherent coupling of the two beams can be decreased by using beams with orthogonal polarizations.

The two contributions to the probe absorption behave differently as the probe frequency is detuned from the pump frequency. Thus one expects the probe-absorption coefficient to have a non-Lorentzian line shape as a function of the detuning of the pump and probe beams. Both the incoherent and coherent contributions to the probe absorption line shape are found to be approximately Lorentzian, where each of the two contributions has a different linewidth. The composite line shape of the probe absorption in the *saturated* medium appears like a double dip as a function of the detuning of the pump and probe beams. This double-dip line shape should be especially apparent when the incoherent and coherent contributions to the probe absorption have linewidths that are significantly different. A double-dip absorption line shape has been observed in p-type Ge for a pump laser with a wavelength of 10.6 μm.[11] In this paper, explicit values are shown for the absorption line shape of a weak tunable probe beam in p-type Ge in the presence of a high-intensity pump beam at 10.6 μm, and good agreement is found with the experiments of Ref. 11.

In addition to the coherent contribution to the probe-beam absorption, the population pulsations can also generate a third optical wave at a frequency $(2\omega_+ - \omega_-)$ with a wave vector $(2\vec{K}_+ - \vec{K}_-)$. Here $\vec{K}_+$ and $\vec{K}_-$ are the wave vectors of the pump and probe beams, respectively. If phase-matching conditions are satisfied, this generated wave can reach an intensity comparable to that of the probe beam. In this paper, we discuss the origin of this generated wave and estimate its intensity as a function of the pump and probe intensities and the detuning between the two optical beams.

Previous theoretical discussions of the absorption of a probe beam have been presented for inhomogeneously broadened atomic systems with a distribution of frequencies at resonance as a result of Doppler broadening.[14–16] Inhomogeneous media which are not velocity broadened have also been considered.[17–19] These calculations have shown the inadequacy of using only the hole-burning model to describe the probe absorption for several different experimental situations. Two theoretical treatments of the probe absorption in p-type Ge have been presented.[9–10] In Refs. 9 and 10, the Ge valence bands were modeled as an ensemble of two-level systems with cascade relaxation. The calculation of Ref. 10 includes only the incoherent contribution to the probe-absorption coefficient, and thus finds the probe absorption line shape to be approximately Lorentzian as a function of the detuning of the pump and probe beams, which is in conflict with the measured results of Ref. 11. The generated wave at $2\omega_+ - \omega_-$ has not been previously discussed for this system. In our calculational approach, the Ge valence bands are described using $\vec{k}\cdot\vec{p}$ theory which includes the nonparabolic and anisotropic valence-band structure. The effect of the interaction of the probe with the saturated medium is described as a perturbation series in the probe-field strength. Detailed results are presented to first order in the probe-field strength.

The paper is organized in the following way: In Sec. II we present our theoretical approach, in Sec. III we give the results for p-type Ge, and in Sec. IV we summarize our conclusions. In Appendix A we describe the effect of the induced current density on the propagation of the optical beams, and in Appendix B we briefly discuss the effect of higher-order terms in the probe field.

II. THEORETICAL APPROACH

In semiconductors with a diamond or zinc-blende structure, there are six bands near the valence-band maximum (three sets of twofold degenerate bands). The heavy- and light-hole bands are degenerate at the zone center and the other two degenerate bands (split-off hole bands) are separated at $k=0$ by the spin-orbit interaction. In thermal equilibrium the occupied hole states are in heavy- and light-hole bands only.

The absorption of light in the 10-μm region by p-type germanium at room temperature is dominated by intervalence-band transitions between the heavy- and light-hole bands.[19,20] Since both energy and wave vector are conserved in the excitation process, only holes in a narrow region of $\vec{k}$ space can directly participate in the optical absorption. At low-light intensities, the relaxation mechanisms maintain the hole distribution near equilibrium. However, as the intensity of the CO_2-laser light becomes sufficiently large, scattering can no longer maintain the distribution at the equilibrium value, and the occupation probabilities for resonant hole states decrease in the heavy-hole band and increase in the light-hole band. Since the absorption is governed by the population difference of these resonant states, this redistribution leads to a reduced absorption coefficient. Thus in order to calculate the absorption of a probe beam in the presence of a saturating beam, one must first calculate the hole distribution in the heavy- and light-hole bands as a function of the intensity of the pump laser.

The calculational approach is to solve for the current density induced by intervalence-band transitions. The equations are constructed by use of a density-matrix formalism. The density matrix of the whole system is written as the product of the density matrix describing the electronic part of the problem and the density matrix describing the lattice system. The lattice is considered to be a surrounding medium and regarded as large and dissipative. Since the lattice (which acts as a heat bath) is not significantly heated over the duration of the optical interaction, the density matrix describing the lattice can be taken to be in thermal equilibrium. By tracing over the lattice modes, the time evolution of the density matrix describing the electronic part of the problem is used to construct equations for the current density. The current density owing to the intervalence-band transitions is found to be determined by[13]

$$\frac{d^2}{dt^2}\vec{J}(\vec{k})+\frac{2}{T_2(\vec{k})}\frac{d}{dt}\vec{J}(\vec{k})+\Omega^2(\vec{k})\vec{J}(\vec{k})=N_h\frac{e^2}{\hbar^2m^2c}\sum_{\substack{b\in h,\\ c\in l}}[f_h(\vec{k})-f_l(\vec{k})]\hbar\Omega(\vec{k})\vec{A}\cdot(\vec{P}_{bc}\vec{P}_{cb}+\vec{P}_{cb}\vec{P}_{bc})\ . \tag{1}$$

Here, $\vec{k}$ is the hole wave vector, h (l) refers to the heavy- (light-) hole band, $\hbar\Omega(\vec{k})$ is the energy difference between states of the wave vector $\vec{k}$ in the heavy- and light-hole bands, $f_i(\vec{k})$ is the one-hole occupation probability for a state with wave vector $\vec{k}$ in band i, A is the vector potential describing the electromagnetic field, $P_{bc}(\vec{k})$ is the momentum matrix element between states with wave vector $\vec{k}$ in bands b and c (which is summed over the twofold-degenerate states in each band), and $\vec{J}(\vec{k})$ is the part of the current density $\vec{J}$ which includes the contribution from states with wave vector $\vec{k}$ [$\sum_{\vec{k}}\vec{J}(\vec{k})=\vec{J}$]. $T_2(\vec{k})$ is given by

$$\frac{2}{T_2(\vec{k})}=\sum_{c,\vec{k}'}(R_{h,\vec{k}\to c,\vec{k}'}+R_{l,\vec{k}\to c,\vec{k}'})\ , \tag{2}$$

where $R_{a,\vec{k}\to b,\vec{k}'}$ is the rate at which a hole in band a with wave vector $\vec{k}$ is scattered into a state with wave vector $\vec{k}'$ in band b. One should note that at low intensity $f_h(\vec{k})-f_l(\vec{k})$ has cubic symmetry so that the current density $\vec{J}$ (after having summed on $\vec{k}$) is parallel to $\vec{A}$. However, at high pump intensities $f_h(\vec{k})-f_l(\vec{k})$ no longer has cubic symmetry, and $\vec{J}(\vec{k})$ [as calculated from Eq. (1)] is not necessarily parallel to $\vec{A}$.

Rate equations for the distribution of hole states are also constructed using the density-matrix formalism. The equations of motion for the distribution functions (for nondegenerate hole densities) are given by[13]

$$\frac{df_h(\vec{k})}{dt}=-\frac{1}{2N_hc\hbar\Omega(\vec{k})}\left[\frac{d}{dt}\vec{J}(\vec{k})\cdot\vec{A}\right]-\sum_{c,\vec{k}'}[R_{h,\vec{k}\to c,\vec{k}'}f_h(\vec{k})-R_{c,\vec{k}'\to h,\vec{k}}f_c(\vec{k}')] \tag{3a}$$

and

$$\frac{df_l(\vec{k})}{dt}=\frac{1}{2N_hc\hbar\Omega(\vec{k})}\left[\frac{d}{dt}\vec{J}(\vec{k})\cdot\vec{A}\right]-\sum_{c,\vec{k}'}[R_{l,\vec{k}\to c,\vec{k}'}f_l(\vec{k})-R_{c,\vec{k}'\to l,\vec{k}}f_c(\vec{k}')]\ . \tag{3b}$$

We consider the case in which the medium is subjected to two electromagnetic waves (pump and probe beams). The high-intensity pump beam is described by a plane wave with polarization $\vec{\eta}_+$, frequency ω_+, and propagation constant $\vec{K}_+$. The low-intensity probe beam is described by a plane wave with polarization $\vec{\eta}_-$, frequency ω_-, and propagation constant $\vec{K}_-$. The vector potential of the electromagnetic field is then given by

$$\vec{A}(\vec{r},t)=\frac{A_+}{2}\vec{\eta}_+(e^{i(\omega_+t-\vec{K}_+\cdot\vec{r})}+\text{c.c.})+\frac{A_-}{2}\vec{\eta}_-(e^{i(\omega_-t-\vec{K}_-\cdot\vec{r})}+\text{c.c.})\ . \tag{4}$$

Using Eq. (4), we wish to solve Eqs. (3a) and (3b) for $f_h(\vec{k})$ and $f_l(\vec{k})$ as a function of the light intensity of the two beams.

In the typical pump-and-probe experiment ($A_+ \gg A_-$), one can write the hole distributions in the heavy- and light-hole bands and the current density as a perturbation expansion in the probe-field magnitude. We define

$$f_h(\vec{k})=f_h^{(0)}(\vec{k})+f_h^{(1)}(\vec{k})+f_h^{(2)}(\vec{k})+\cdots\ , \tag{5a}$$

$$f_l(\vec{k})=f_l^{(0)}(\vec{k})+f_l^{(1)}(\vec{k})+f_l^{(2)}(\vec{k})+\cdots\ , \tag{5b}$$

and

$$\vec{J}(\vec{k})=\vec{J}^{(0)}(\vec{k})+\vec{J}^{(1)}(\vec{k})+\vec{J}^{(2)}(\vec{k})+\cdots\ . \tag{5c}$$

The zero-order terms designate the occupation probabilities and current density for the medium subject to the saturating beam and no probe laser. The first-order terms represent the modification due to the presence of the probe beam (to first order in the probe-field strength). The higher-order terms are defined in an analogous way. For small probe-field strengths, the expansion can be truncated at first order in the calculation of the probe absorption coefficient. In order to use a perturbation expansion in the probe-field strength, one requires that the probe intensity be much smaller than the saturation intensity of the material ($\sim$4 MW/cm^2 in p-type Ge at room temperature).

By substituting the expanded forms of Eqs. 5(a)—5(c) into the governing equations for the current density given by Eq. (1) and for the hole-occupation probabilities given by Eqs. (3a) and (3b), $f_h^{(0)}$ and $f_l^{(0)}$ are found to be independent of time and space, and $f_h^{(1)}(\vec{k})$, $f_l^{(1)}(\vec{k})$, $\vec{J}^{(0)}(\vec{k})$, and $\vec{J}^{(1)}(\vec{k})$ are found to oscillate as

$$f_h^{(1)}(\vec{k})=F_h^{(1)}(\vec{k})\exp i[(\omega_+-\omega_-)t-(\vec{K}_+-\vec{K}_-)\cdot\vec{r}]+\text{c.c.}\ , \tag{6a}$$

$$f_l^{(1)}(\vec{k})=F_l^{(1)}(\vec{k})\exp i[(\omega_+-\omega_-)t-(\vec{K}_+-\vec{K}_-)\cdot\vec{r}]+\text{c.c.}\ , \tag{6b}$$

$$\vec{J}^{(0)}(\vec{k})=\vec{R}^{(0)}(\vec{k})\exp i[\omega_+t-\vec{K}_+\cdot\vec{r}]+\text{c.c.}\ , \tag{6c}$$

and

$$\vec{J}^{(1)}(\vec{k})=(\vec{R}^{(1)}(\vec{k})\exp\{i[(2\omega_+-\omega_-)t-(2\vec{K}_+-\vec{K}_-)\cdot\vec{r}]\}+\text{c.c.})+(\vec{I}^{(1)}(\vec{k})\exp\{i[\omega_- t-\vec{K}_-\cdot\vec{r}]\}+\text{c.c.}) . \tag{6d}$$

In the above equations, we have dropped terms in the hole-occupation probabilities which oscillate at frequency 2ω. These high-frequency oscillations are highly damped by the scattering terms.

The first-order terms in $f_h(\vec{k})$ and $f_l(\vec{k})$ describe a pulsation in the population of free holes due to a forcing oscillation at the beat frequency Δ ($\Delta=\omega_+-\omega_-$). This population pulsation is due to a nonlinear coupling of the free-hole distribution to the two laser beams with frequencies ω_+ and ω_-. This interaction is described by the $[d\vec{J}(\vec{k})/dt]\cdot\vec{A}$ terms of Eqs. (3a) and (3b), in which $\vec{J}(\vec{k})$ is driven at one of the frequencies and the component of $\vec{A}$ is oscillating at the other frequency. The first term in Eq. (6d) arises from the first-order oscillating (frequency Δ) contribution to the population difference $f_h(\vec{k})-f_l(\vec{k})$ mixing with the pump component of $\vec{A}$ (oscillating at ω_+) in Eq. (1). The second term in Eq. (6d) arises from both the zeroth-order steady-state contribution to the population difference (f_h-f_l) mixing with the probe contribution of $\vec{A}$ (i.e., the hole-burning contribution) and from the first-order oscillating contribution to f_h-f_l mixing with the pump contribution of $\vec{A}$ in Eq. (1).

The solution to the zeroth-order equations (i.e., for $A_-=0$) has previously been investigated by the authors.[13] The results of Ref. 13 are briefly summarized since they will be used later in calculating the probe absorption coefficient. $\vec{R}^{(0)}(\vec{k})$ in the current-density expression [Eq. (6c)] is given by

$$\vec{R}^{(0)}(\vec{k})=\frac{A_+}{2}\frac{N_h e^2}{\hbar m^2 c}\frac{1}{\Omega(\vec{k})-\omega_++i/T_2}[f_h^{(0)}(\vec{k})-f_l^{(0)}(\vec{k})]\left[\frac{1}{2}\sum_{\substack{b\in h,\\ c\in l}}\vec{\eta}_+\cdot(\vec{P}_{bc}\vec{P}_{cb}+\vec{P}_{cb}\vec{P}_{bc})\right] , \tag{7}$$

where

$$f_h^{(0)}(\vec{k})-f_l^{(0)}(\vec{k})=\frac{f_h^e(\vec{k})-f_l^e(\vec{k})+T_h(\vec{k})F(\vec{k})-T_l(\vec{k})G(\vec{k})}{1+\beta(\vec{k})[T_h(\vec{k})+T_l(\vec{k})]} . \tag{8}$$

In Eq. (8), $f_c^e(\vec{k})$ is the equilibrium value of the distribution for a state with wave vector $\vec{k}$ in band c, and the following auxiliary functions are introduced to simplify the expressions for $f_h^{(0)}(\vec{k})$ and $f_l^{(0)}(\vec{k})$:

$$\frac{1}{T_h(\vec{k})}=\sum_{c,\vec{k}'}R_{h,\vec{k}\to c,\vec{k}'} , \tag{9a}$$

$$\frac{1}{T_l(\vec{k})}=\sum_{c,\vec{k}'}R_{l,\vec{k}\to c,\vec{k}'} , \tag{9b}$$

$$F(\vec{k})=\sum_{c,\vec{k}'}R_{c,\vec{k}'\to h,\vec{k}}[f_c^{(0)}(\vec{k}')-f_c^e(\vec{k}')] , \tag{9c}$$

$$G(\vec{k})=\sum_{c,\vec{k}'}R_{c,\vec{k}'\to l,\vec{k}}[f_c^{(0)}(\vec{k}')-f_c^e(\vec{k}')] , \tag{9d}$$

and

$$\beta(\vec{k})=\frac{2\pi^2}{\sqrt{\epsilon}m^2\omega c}\frac{e^2 I_+}{\hbar\omega}\sum_{\substack{b\in h,\\ c\in l}}|\vec{\eta}_+\cdot\vec{P}_{bc}(\vec{k})|^2\frac{1/[\pi\hbar T_2(\vec{k})]}{[\Omega(\vec{k})-\omega_+]^2+[1/T_2(\vec{k})]^2} , \tag{9e}$$

where I_+ is the intensity of the pump laser.

By using Maxwell's equations and Eq. (7), an expression can be written (see Appendix A) for the absorption coefficient of the pump beam. By solving for the difference in the occupation probabilities for states in the resonant region using Eq. (8), one can calculate the absorption coefficient of the pump as a function of the pump intensity. The results are presented in Refs. 13 and 21 and are found to be in good agreement with the experimental measurements of Refs. 2–6.

We now derive expressions for the first-order results for $f_h(\vec{k})-f_l(\vec{k})$ and $\vec{J}^{(1)}(\vec{k})$. Substituting the expansion defined by Eq. (5) into Eq. (1), and equating terms to first order in the probe-field strength, one finds

$$\frac{d}{dt^2}\vec{\mathrm{J}}^{(1)}(\vec{\mathrm{k}})+\frac{2}{T_2(\vec{\mathrm{k}})}\frac{d}{dt}\vec{\mathrm{J}}^{(1)}(\vec{\mathrm{k}})+\Omega^2(\vec{\mathrm{k}})\vec{\mathrm{J}}^{(1)}(\vec{\mathrm{k}})$$

$$=N_h\frac{e^2}{\hbar^2m^2c}\sum_{\substack{b\in h,\\ c\in l}}\left\{\left\{[f_h^{(0)}(\vec{\mathrm{k}})-f_l^{(0)}(\vec{\mathrm{k}})]\hbar\Omega(\vec{\mathrm{k}})[\vec{\eta}_-\cdot\vec{\mathrm{P}}_{bc}(\vec{\mathrm{k}})\vec{\mathrm{P}}_{cb}(\vec{\mathrm{k}})+\vec{\eta}_-\cdot\vec{\mathrm{P}}_{cb}(\vec{\mathrm{k}})\vec{\mathrm{P}}_{bc}(\vec{\mathrm{k}})]\frac{A_-}{2}(e^{i(\omega_-t-\vec{\mathrm{K}}_-\cdot\vec{\mathrm{r}})}+\text{c.c.})\right\}\right.$$

$$\left.+\left\{[f_h^{(1)}(\vec{\mathrm{k}})-f_l^{(1)}(\vec{\mathrm{k}})]\hbar\Omega(\vec{\mathrm{k}})[\vec{\eta}_+\cdot\vec{\mathrm{P}}_{bc}(\vec{\mathrm{k}})\vec{\mathrm{P}}_{cb}(\vec{\mathrm{k}})+\vec{\eta}_+\cdot\vec{\mathrm{P}}_{cb}(\vec{\mathrm{k}})\vec{\mathrm{P}}_{bc}(\vec{\mathrm{k}})]\times\frac{A_+}{2}(e^{i(\omega_+t-\vec{\mathrm{K}}_+\cdot\vec{\mathrm{r}})}+\text{c.c.})\right\}\right\}, \tag{10}$$

for the first-order correction to the current density due to the presence of the probe. Substitution of the expansion into Eq. (3) yields the following expressions for $f_h^{(1)}(\vec{\mathrm{k}})$ and $f_l^{(1)}(\vec{\mathrm{k}})$:

$$\frac{df_h^{(1)}(\vec{\mathrm{k}})}{dt}=\frac{-1}{2N_hc\hbar\Omega}\left\{\left[\left(\frac{d}{dt}\vec{\mathrm{J}}^{(0)}(\vec{\mathrm{k}})\right)\cdot\vec{\eta}_-\frac{A_-}{2}(e^{i(\omega_-t-\vec{\mathrm{K}}_-\cdot\vec{\mathrm{r}})}+\text{c.c.})\right.\right.$$

$$\left.\left.+\left(\frac{d}{dt}\vec{\mathrm{J}}^{(1)}(\vec{\mathrm{k}})\right)\cdot\vec{\eta}_+\frac{A_+}{2}(e^{i(\omega_+t-\vec{\mathrm{K}}_+\cdot\vec{\mathrm{r}})}+\text{c.c.})\right]\right\}$$

$$-\sum_{c,\vec{\mathrm{k}}'}[R_{h,\vec{\mathrm{k}}\to c,\vec{\mathrm{k}}'}f_h^{(1)}(\vec{\mathrm{k}})-R_{c,\vec{\mathrm{k}}'\to h,\vec{\mathrm{k}}}f_c^{(1)}(\vec{\mathrm{k}}')] \tag{11a}$$

and

$$\frac{df_l^{(1)}(\vec{\mathrm{k}})}{dt}=\frac{1}{2N_hc\hbar\Omega}\left\{\left[\left(\frac{d}{dt}\vec{\mathrm{J}}^{(0)}(\vec{\mathrm{k}})\right)\cdot\vec{\eta}_-\frac{A_-}{2}(e^{i(\omega_-t-\vec{\mathrm{K}}_-\cdot\vec{\mathrm{r}})}+\text{c.c.})\right.\right.$$

$$\left.\left.+\left(\frac{d}{dt}\vec{\mathrm{J}}^{(1)}(\vec{\mathrm{k}})\right)\cdot\vec{\eta}_+\frac{A_+}{2}(e^{i(\omega_+t-\vec{\mathrm{K}}_+\cdot\vec{\mathrm{r}})}+\text{c.c.})\right]\right\}$$

$$-\sum_{c,\vec{\mathrm{k}}'}[R_{l,\vec{\mathrm{k}}\to c,\vec{\mathrm{k}}'}f_l^{(1)}(\vec{\mathrm{k}})-R_{c,\vec{\mathrm{k}}'\to l,\vec{\mathrm{k}}}f_c^{(1)}(\vec{\mathrm{k}}')]\,. \tag{11b}$$

Using Eq. (6) in Eqs. (10) and (11), one can write expressions for $F_h^{(1)}(\vec{\mathrm{k}})-F_l^{(1)}(\vec{\mathrm{k}})$, $\vec{\mathrm{R}}^{(1)}(\vec{\mathrm{k}})$, and $\vec{\mathrm{I}}^{(1)}(\vec{\mathrm{k}})$ by equating terms which oscillate with the same spatial and temporal dependence. After equating coefficients one finds

$$F_h^{(1)}(\vec{\mathrm{k}})-F_l^{(1)}(\vec{\mathrm{k}})=\frac{-i/T_2(\vec{\mathrm{k}})}{[\Omega(\vec{\mathrm{k}})-\omega_-]+[i/T_2(\vec{\mathrm{k}})]}\left[\frac{A_-}{A_+}\right][f_h^{(0)}(\vec{\mathrm{k}})-f_l^{(0)}(\vec{\mathrm{k}})]$$

$$\times\frac{I_+B^*}{l(\vec{\mathrm{k}})}\frac{\sum_{\substack{b\in h,\\ c\in l}}[(\vec{\mathrm{P}}_{bc}\cdot\vec{\eta}_+)(\vec{\mathrm{P}}^*_{bc}\cdot\vec{\eta}_-)+\text{c.c.}]}{2\sum_{\substack{b\in h,\\ c\in l}}|\vec{\eta}_+\cdot\vec{\mathrm{P}}_{bc}|^2}, \tag{12}$$

$$\vec{\mathrm{R}}^{(1)}(\vec{\mathrm{k}})=\frac{-iA_-}{2}\frac{1/(\pi\hbar T_2)}{(\Omega-\omega_-)^2+(1/T_2)^2}\frac{\pi N_he^2}{m^2c}[f_h^{(0)}(\vec{\mathrm{k}})-f_l^{(0)}(\vec{\mathrm{k}})]\frac{I_+B^*}{l(\vec{\mathrm{k}})}\left[\frac{(\Omega-\omega_-)-(i/T_2)}{\Omega-(2\omega_+-\omega_-)+(i/T_2)}\right]$$

$$\times\left[\tfrac{1}{2}\sum_{\substack{b\in h,\\ c\in l}}\vec{\eta}_+\cdot(\vec{\mathrm{P}}_{bc}\vec{\mathrm{P}}_{cb}+\text{c.c.})\right]\frac{\sum_{\substack{b\in h,\\ c\in l}}[(\vec{\mathrm{P}}_{bc}\cdot\vec{\eta}_+)(\vec{\mathrm{P}}^*_{bc}\cdot\vec{\eta}_-)+\text{c.c.}]}{2\sum_{\substack{b\in h,\\ c\in l}}|\vec{\eta}_+\cdot\vec{\mathrm{P}}_{bc}|^2}, \tag{13}$$

and

$$\vec{I}^{(1)}(\vec{k})=\frac{-iA_-}{2}\frac{1/(\pi\hbar T_2)}{(\Omega-\omega_-)+(1/T_2)^2}\frac{\pi N_h e^2}{m^2 c}[f_h^{(0)}(\vec{k})-f_l^{(0)}(\vec{k})]$$
$$\times\left\{[1+iT_2(\Omega-\omega_-)]\left[\frac{1}{2}\sum_{\substack{b\in h,\\ c\in l}}\vec{\eta}_-\cdot(\vec{P}_{bc}\vec{P}_{cb}+\text{c.c.})\right]-\frac{I_+B}{l(\vec{k})}\left[\frac{1}{2}\sum_{\substack{b\in h,\\ c\in l}}\vec{\eta}_+\cdot(\vec{P}_{bc}\vec{P}_{cb}+\text{c.c.})\right]\right.$$
$$\left.\times\frac{\sum_{\substack{b\in h,\\ c\in l}}[(\vec{P}_{bc}\cdot\vec{\eta}_+)(\vec{P}^*_{bc}\cdot\vec{\eta}_-)+\text{c.c.}]}{2\sum_{\substack{b\in h,\\ c\in l}}|\vec{\eta}_+\cdot\vec{P}_{bc}|^2}\right\}. \tag{14}$$

In the equations above, the auxillary functions $l(\vec{k})$ and $B(\vec{k})$ are introduced to simplify the expressions. The functions are defined by

$$l(\vec{k})=\frac{\hbar^2 c\sqrt{\epsilon}m^2\omega_+^2}{2\pi e^2\sum_{\substack{b\in h,\\ c\in l}}|\vec{\eta}_+\cdot\vec{P}_{bc}|^2 T_2(T_h+T_l)} \tag{15a}$$

and

$$B(\vec{k})=\frac{[1/T_2+i(\Omega-\omega_-)]\left[\dfrac{1}{1/T_2-i(\Omega-\omega_-)}+\dfrac{1}{1/T_2+i(\Omega-\omega_+)}\right]}{2\mathcal{J}(\vec{k})+\dfrac{I_+}{l(\vec{k})}\dfrac{1}{T_2}\left[\dfrac{1}{1/T_2-i(\Omega-\omega_-)}+\dfrac{1}{1/T_2+i(\Omega-2\omega_++\omega_-)}\right]}, \tag{15b}$$

where

$$\mathcal{J}(\vec{k})=\frac{T_h(\vec{k})+T_l(\vec{k})}{\dfrac{1}{1/T_h+i(\omega_+-\omega_-)}+\dfrac{1}{1/T_l-i(\omega_+-\omega_-)}}, \tag{15c}$$

and $T_h(\vec{k})$ and $T_l(\vec{k})$ are defined by Eqs. (9a) and (9b). In deriving these results, we have included the term $\sum_{c,\vec{k}'}R_{c,\vec{k}'\to h,\vec{k}}f_c(\vec{k}',t)$ in Eq. (3a) and the corresponding term in Eq. (3b) only to zeroth order (thus it does not enter into the equation for the higher-order results). These terms correspond to scattering of holes from states primarily outside the resonant region into states in the resonant region. The population of the states outside the resonant region is not significantly affected by the presence of the probe beam. We have also assumed that the frequencies ω_+, ω_-, and Ω are nearly equal.

Using the expressions for the first-order correction to the current density and the wave equation, one finds how the electromagnetic wave propagation is influenced by $\vec{J}^{(1)}$. The details of this analysis are contained in Appendix A. To first order in the probe-field strength, the propagation of the pump beam is not influenced by the probe beam. (The first contribution to a modification of the pump beam is second order in the probe field.) This result is immediately obvious from the form of $\vec{J}^{(1)}$ in Eq. (6d), because it does not contain a term which oscillates as $\omega_+t-\vec{K}_+\cdot\vec{r}$. The propagation of the probe beam is influenced by the term $\vec{I}^{(1)}$ in $\vec{J}^{(1)}$. In Eq. (14) for $\vec{I}^{(1)}(\vec{k})$, the first term in the large square brackets describes the usual absorption of the probe beam as modified by the saturating beam through the intensity dependence of the distribution functions $f_h^{(0)}(\vec{k})-f_l^{(0)}(\vec{k})$. The second term in large square brackets of Eq. (14) (i.e., the term proportional to I_+) describes the coherent coupling between the pump and probe beams. The $\vec{R}^{(1)}$ term in $\vec{J}^{(1)}$ leads to the generation of a third optical beam which oscillates at $(2\omega_+-\omega_-)t-(2\vec{K}_+-\vec{K}_-)\cdot\vec{r}$. This beam can reach intensities comparable to that of the probe beam if phase matching conditions are satisfied.

In Appendix A we find that the absorption coefficient of the probe beam is given by

$$\alpha_-(\omega_-,I_+)=-\sum_{\vec{k}}\frac{8\pi\,\mathrm{Im}[\vec{I}^{(1)}(\vec{k})\cdot\vec{\eta}_-]}{cK_-A_-}, \tag{16a}$$

which can be rewritten as

$$\alpha_-(\omega_-,I_+)=\frac{4\pi^2N_he^2}{\sqrt{\epsilon}m^2c\omega_-}\sum_{\vec{k}}\left[\sum_{\substack{b\in h,\\ c\in l}}|\vec{\eta}_-\cdot\vec{P}_{bc}(\vec{k})|^2\right][f_h^{(0)}(\vec{k})-f_l^{(0)}(\vec{k})]\frac{1/[\pi\hbar T_2(\vec{k})]}{[\Omega(\vec{k})-\omega_-]^2+[1/T_2(\vec{k})]^2}$$
$$\times\left[1-\frac{I_+}{l(\vec{k})}\mathrm{Re}[B(\vec{k})]\frac{\left[\sum_{\substack{b\in h,\\ c\in l}}\{[\vec{\eta}_+\cdot\vec{P}_{bc}(\vec{k})][\vec{\eta}_-\cdot\vec{P}^*_{bc}(\vec{k})]+\text{c.c.}\}\right]^2}{4\sum_{\substack{b\in h,\\ c\in l}}|\vec{\eta}_+\cdot\vec{P}_{bc}(\vec{k})|^2\sum_{\substack{b\in h,\\ c\in l}}|\vec{\eta}_-\cdot\vec{P}_{bc}(\vec{k})|^2}\right]. \tag{16b}$$

The unity term in the brackets of Eq. (16b) gives the usual contribution to the probe absorption coefficient modified by the hole-burning effect of the pump beam (i.e., the distribution functions $f_h^{(0)}(\vec{k})-f_l^{(0)}(\vec{k})$ are modified by the pump beam). The second term in the brackets, which is proportional to I_+, describes the effect of the coherent coupling of the pump and probe beams on the probe absorption coefficient. It comes about because of the oscillations in the difference in occupation probabilities for states in the resonant region of the heavy- and light-hole bands, which is described by $f_h^{(1)}(\vec{k})-f_l^{(1)}(\vec{k})$. For beat frequencies Δ (equal to $\omega_+-\omega_-$) much less than $1/T_h(\vec{k})$ and $1/T_l(\vec{k})$, the contribution due to the coherent coupling of the two beams can be comparable to the contribution from the hole-burning term. As the beat frequency is increased so that Δ is comparable to the scattering rates, the contribution from the coherent coupling term decreases and this contribution becomes vanishingly small for Δ significantly greater than the scattering rates. It is interesting to notice that the coherent coupling term does not vanish for orthogonally polarized pump and probe beams (although it is significantly less for the orthogonally polarized case than for the parallel polarized case).

In Appendix A, the term $\vec{R}^{(1)}$ in the current-density expression is shown to lead to the generation of a third optical beam which oscillates as $(2\omega_+-\omega_-)t-(2\vec{K}_+-\vec{K}_-)\cdot\vec{r}$. The intensity of this generated beam will be very weak unless $\vec{K}_+$ and $\vec{K}_-$ are nearly parallel (i.e., the pump and probe beams are nearly unidirectional). If $\vec{K}_+$ and $\vec{K}_-$ are nearly parallel, a rough estimate of the intensity of the generated beam (given in Appendix A) shows that it can reach approximately a factor of ξ times the intensity of the incident probe beam where

$$\xi=\left|\frac{[\bar{\vec{R}}^{(1)}\cdot\vec{\eta})/A_-}{\frac{2(\bar{\vec{R}}^{(0)}\cdot\vec{\eta}_+)}{A_+}-\left[\frac{\bar{\vec{I}}^{(1)}\cdot\vec{\eta}_-}{A_-}\right]^*+\frac{\epsilon\omega^2}{2\pi c}(1-\cos\theta)}\right|^2. \tag{17}$$

Here the bar over the current-density components indicates a sum on $\vec{k}$ [i.e., $\vec{R}^{(0)}=\sum_{\vec{k}}\vec{R}^{(0)}(\vec{k})$, etc.], $\vec{\eta}$ is a unit vector in the direction of $\vec{R}^{(1)}$, and θ is the angle (assumed small) between $\vec{K}_+$ and $\vec{K}_-$. This expression can be used to estimate the maximum intensity of the generated beam as a function of $\omega_+-\omega_-$, the pump-beam intensity, and the angle θ.

The inclusion of higher-order terms in the probe-field strength leads to a modification of the pump beam and to the generation of additional side bands at plus or minus integral multiples of the beat frequency Δ from the pump frequency. A short discussion of these higher-order terms is included in Appendix B.

III. RESULTS AND DISCUSSION

In this section we present results for the first-order correction to the population difference for states near the resonant region, the effect of relative pump-and-probe polarizations on the nonlinear coupling of the two beams, the effect of the nonlinear coupling on the probe absorption, and the probe absorption as a function of the detuning of the pump and probe beams. At the end of this section, a discussion is presented on the strength of the new wave generated with frequency $2\omega_+-\omega_-$ as a function of the probe frequency and pump intensity. In order to calculate the quantities of interest, one must first calculate $f_h^{(0)}(\vec{k})$, $f_l^{(0)}(\vec{k})$, and $\vec{R}^{(0)}(\vec{k})$ in the case with only the pump beam present. The calculational approach proceeds as discussed in Ref. 13. The one-hole energies and momentum matrix elements appearing in the equations are determined by second-order degenerate $\vec{k}\cdot\vec{p}$ perturbation theory.[22] The cyclotron resonance parameters of Ref. 23 are used in calculating the valence-band structure and momentum matrix elements. The hole-phonon scattering is the dominant relaxation mechanism at room temperature for hole concentrations less than about 3×10^{15} cm^{-3}. The hole-phonon scattering rates are calculated on the basis of the deformable potential model as discussed in Refs. 24 and 25. For more heavily doped samples, the hole-hole and hole-ionized impurity are included following Ref. 26. By using the calculated scattering rates, the scattering times $T_2(\vec{k})$, $T_h(\vec{k})$, and $T_l(\vec{k})$ are computed from Eqs. (2), (9a), and (9b). Having calculated the hole energies, momentum matrix elements, scattering times, and occupation probabilities as a function of wave vector $\vec{k}$, one can perform the numerical integration over $\vec{k}$ space to determine the probe absorption coefficient in the presence of the high-intensity pump laser.

Only hole-phonon scattering is included in most of the calculated results presented in this section. For hole densities in which hole-hole and hole-ionized impurity scattering becomes important ($N_h \gtrsim 3\times10^{15}$ cm^{-3}), the calculated results depend on the particular choice of hole concentration. Rather than specifying the hole concentration in each figure, we present results in the low-density limit. The transmission experiments of Ref. 11 which measure $\alpha_-(\omega_-,I_+)$ were performed on moderately doped samples where one should also include hole-hole and hole-impurity scattering. The values of $\alpha_-(\omega_-,I_+)$, which are compared with experiment in this section, are calculated at the particular value of the hole concentration corresponding to the samples used in the experiment.

Both the coherent interaction between pump and probe beams and the generated wave at $2\omega_+-\omega_-$ result from the first-order correction to the population difference $(f_h^{(1)}(\vec{k})-f_l^{(1)}(\vec{k}))$, which oscillates as $(\omega_+-\omega_-)t-(\vec{K}_+-\vec{K}_-)\cdot\vec{r})$. The magnitude of this population difference is calculated from Eq. (12). In Fig. 1, we plot

$$Q(\vec{k})=\frac{-[F_h^{(1)}(\vec{k})-F_l^{(1)}(\vec{k})]}{f_h^{(0)}(\vec{k})-f_l^{(0)}(\vec{k})}\sqrt{I_+/I_-}\ , \tag{18}$$

as a function of $\hbar\Omega(\vec{k})$ for $\vec{k}$ in the [111] direction for two pump intensities. Both pump and probe beams are taken to have photon energies of 117 meV (e.g., $\lambda=10.6$ μm) and to be polarized in the [001] direction. For zero beat frequency ($\Delta=\omega_+-\omega_-=0$), Q is purely real. For $\vec{k}$ in the [111] direction, values of $I(\vec{k})$ in Eq. (12) are in the range of 5.0–6.5 MW/cm^2 over the region in $\vec{k}$ space shown in Fig. 1. From Fig. 1, we see that the magnitude of the population pulsation increases with increasing intensity. In addition, the magnitude of $F_h^{(0)}(\vec{k})-F_l^{(0)}(\vec{k})$ at zero beat frequency is a maximum for states nearly resonant [i.e., photon energy $\simeq\hbar\Omega(\vec{k})$] and decreases for states which are farther away from the resonant region. For zero beat frequency, the values of Q as a function of $\hbar\Omega(\vec{k})$ have approximately a Lorentzian line shape for states near the resonant region.

For nonzero beat frequency, the structure of $F_h^{(1)}(\vec{k})-F_l^{(1)}(\vec{k})$ vs $\hbar\Omega(\vec{k})$ becomes more complicated, and the imaginary part becomes nonzero. In Fig. 2, the real and imaginary parts Q are shown for a pump beam at 10.6 μm with an intensity of 10 MW/cm^2. The results are for a beat frequency $\Delta=-6.07\times10^{12}$ sec^{-1}, which corresponds to a probe photon energy of 121 meV. Both the pump and probe beams are polarized in the [001] direction. The solid curve shows the real part of Q, and the dashed curve shows the imaginary part. As the pump and probe beams are detuned, the real part of Q has two peaks located at $\hbar\Omega(\vec{k})\simeq\hbar\omega_+$ and $\hbar\Omega(\vec{k})\simeq\hbar\omega_-$. For this value of Δ, the imaginary part has a peak located between $\hbar\omega_+$ and $\hbar\omega_-$ and has approximately a Lorentzian line shape over the range of $\hbar\Omega(\vec{k})$ shown in Fig. 2. For larger detuning of the pump and probe beams, the imaginary part also develops two distinct peaks as a function of $\hbar\Omega(\vec{k})$. The effect of increasing the detuning of the beams is to decrease the magnitude of the maximum value of $F_h^{(1)}(\vec{k})-F_l^{(1)}(\vec{k})$ and to shift the positions at which the peaks occur.

The relative polarization of the pump and probe beams are important in determining the strength of the coherent interaction between the beams. From Eq. (16) we see that the relative polarization dependence is described by

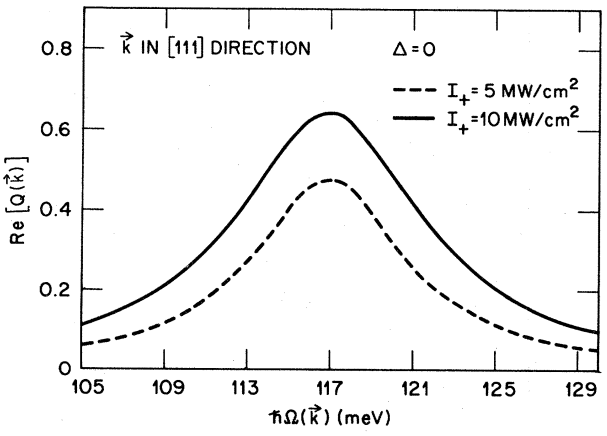

FIG. 1. Calculated values for Re$Q(\vec{k})$ as a function of $\hbar\Omega(\vec{k})$ for $\vec{k}$ in the [111] direction. Both the pump and probe beams are taken to have a wavelength of 10.6 μm, and both beams are polarized in the [001] direction. The dashed curve is for a pump intensity of 5 MW/cm^2, and the solid curve is for a pump intensity of 10 MW/cm^2.

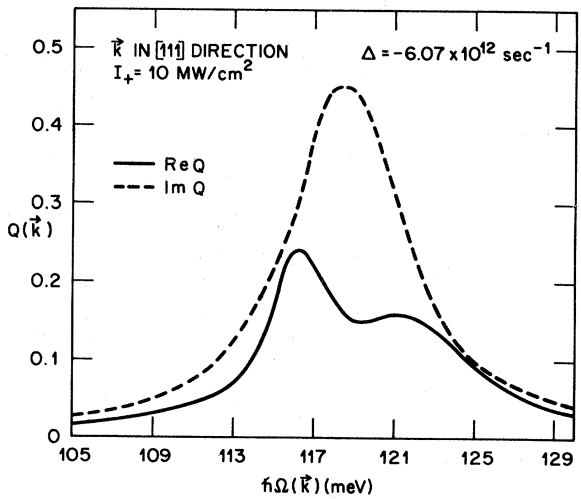

FIG. 2. Calculated values for the real and imaginary parts of Q as a function of $\hbar\Omega(\vec{k})$ for $\vec{k}$ in the [111] direction. The pump beam is taken to have a photon energy of 117 meV, and the probe beam is taken to have a photon energy of 121 meV (i.e., $\Delta=-6.07\times10^{12}$ sec^{-1}). Both beams are taken to be polarized in the [001] direction. The dashed (solid) curve shows the real (imaginary) part of Q for a pump intensity of 10 MW/cm^2.

$$\Xi(\vec{\eta}_+,\vec{\eta}_-,I_+)=\left[\sum_{\vec{k}}\left[\sum_{\substack{b\in h,\\ c\in l}}|\vec{\eta}_-\cdot\vec{P}_{bc}(\vec{k})|^2\right][f_h^{(0)}(\vec{k})-f_l^{(0)}(\vec{k})]\left[\frac{1/(\pi\hbar T_2)}{(\Omega-\omega_-)^2+(1/T_2)^2}\right]\frac{I_+}{l(\vec{k})}\right.$$

$$\left.\times\mathrm{Re}[B(\vec{k})]\frac{\left[\sum_{\substack{b\in h,\\ c\in l}}[\vec{P}_{bc}\cdot\vec{\eta}_+)(\vec{P}^*_{bc}\cdot\vec{\eta}_-)+\text{c.c.}]\right]^2}{4\sum_{\substack{b\in h,\\ c\in l}}|\vec{P}_{bc}\cdot\vec{\eta}_+|^2\sum_{\substack{b\in h,\\ c\in l}}|\vec{P}_{bc}\cdot\vec{\eta}_-|^2}\right]$$

$$\times\left[\sum_{\vec{k}}\left[\sum_{\substack{b\in h,\\ c\in l}}|\vec{\eta}_-\cdot\vec{P}_{bc}|^2\right][f_h^{(0)}(\vec{k})-f_l^{(0)}(\vec{k})]\left[\frac{1/(\pi\hbar T_2)}{(\Omega-\omega_-)^2+(1/T_2)^2}\right]\frac{I_+}{l(\vec{k})}\mathrm{Re}[B(\vec{k})]\right]^{-1}. \quad (19)$$

Values for $\Xi(\omega_+,\omega_-,I_+)$ are shown in Fig. 3 for $\hbar\omega_+=\hbar\omega_-=117$ meV as a function of the relative angle of polarization between the pump and probe beams. In the calculation $\vec{\eta}_+$ is fixed to be in the [001] direction and $\vec{\eta}_-$ is rotated in the x-z plane for angles of rotation from 0—90° (i.e., $\vec{\eta}_-$ is rotated about the y axis from the [001] direction to the [100] direction). The solid line in Fig. 3 is for a pump intensity of 1 MW/cm^2, and the dashed line is for a pump intensity of 20 MW/cm^2. The difference between the two curves is contained in the angular population effects of $f_h^{(0)}(\vec{k})-f_l^{(0)}(\vec{k})$. We note that the nonlinear coupling is at a maximum value when the pump and probe beams are polarized in the same direction, and that the coupling decreases monotonically as the angle between the polarization directions is increased. The coupling does not vanish even in the case of orthogonal polarizations, although it is decreased by about a factor of 5. This suggests that for a transmission measurement in which one attempts to use a probe beam to investigate the modification of the carrier distribution in the vicinity of a saturable resonant transition, one should use a probe polarization which is orthogonal to the polarization of the saturable beam, thereby minimizing the nonlinear coupling of the two beams.

For parallel pump and probe polarizations, the correction to the hole-burning model for $\alpha_-(\omega_-,I_+)$ is contained in the factor $1-I_+/I(\vec{k})\mathrm{Re}B(\vec{k})$ in Eq. (16). This factor depends on the wave vector $\vec{k}$ due to the anisotropy in the valence-band structure. In Fig. 4, the calculated values of $1-I_+/I(\vec{k})\mathrm{Re}B(\vec{k})$ are shown as a function of $\hbar\Omega(\vec{k})$ for $\vec{k}$ in the [111] direction. The top figure is for zero detuning of the two beams ($\hbar\omega_+=\hbar\omega_-=117$ meV) and parallel polarizations ($\vec{\eta}_+||\vec{\eta}_-||$ [001]). The solid curve is for a pump intensity of 1 MW/cm^2, and the dashed curve is for a pump intensity of 10 MW/cm^2. For $\Delta=0$, all values of $1-I_+/I(\vec{k})\mathrm{Re}B(\vec{k})$ are less than unity for states nearly resonant with the pump and probe beams, thus the nonlinear coupling of the beams leads to a decrease in the probe absorption coefficient. The contribution of the nonlinear coupling from states in $\vec{k}$ space is largest for states near resonance and becomes small for

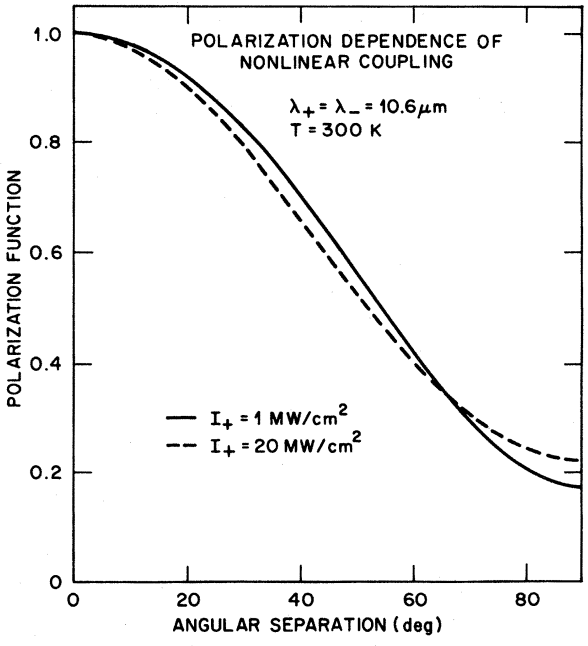

FIG. 3. Calculated values for the polarization function Ξ as a function of the angular separation between the polarizations of the pump and probe beams. Both beams are taken to have a wavelength of 10.6 μm. Here, $\vec{\eta}_+$ is taken to be fixed in the [001] direction, and $\vec{\eta}_-$ rotated in the x-z plane from 0° to 90°. The solid curve is for a pump intensity of 1 MW/cm^2, and the dashed curve is for a pump intensity of 20 MW/cm^2.

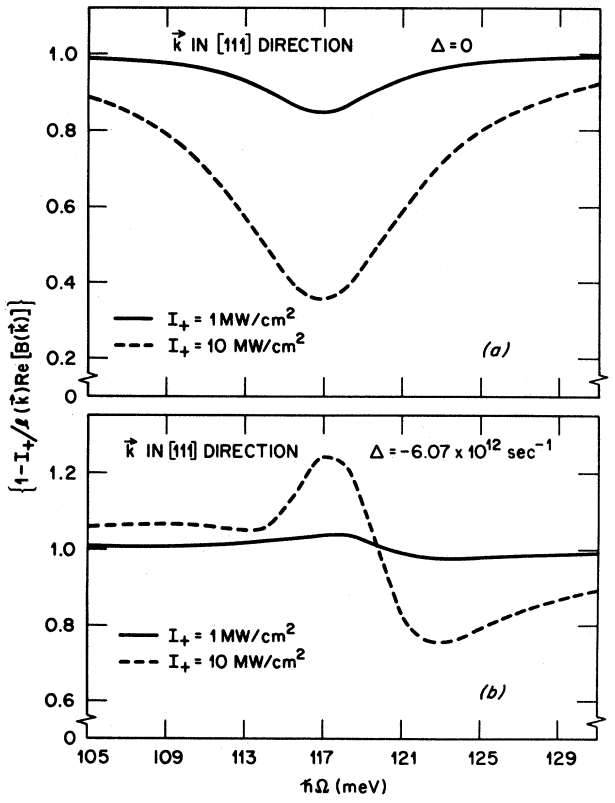

FIG. 4. Calculated values for $1-I_+/I(\vec{k})\mathrm{Re}B(\vec{k})$ as a function of $\hbar\Omega(\vec{k})$ for $\vec{k}$ in the [111] direction. The polarizations of the pump and probe beams are taken to be in the [001] direction. In the top figure, the pump and probe beams are taken to have a photon energy of 117 meV. In the bottom figure, the pump beam is taken to have a photon energy of 117 meV (i.e., $\lambda_+=10.6\ \mu$m) and the probe beam is taken to have a photon energy of 121 meV (i.e., $\Delta=-6.07\times10^{12}$ sec^{-1}). In each figure, the solid (dashed) curve is for a pump intensity of 1 MW/cm^2 (10 MW/cm^2).

states with $\hbar\Omega(\vec{k})$ out of the resonant region.

The effect of detuning the pump and probe beams on the calculated values of $1-I_+/I(\vec{k})\mathrm{Re}B(\vec{k})$ is shown by the bottom illustration in Fig. 4. Here, values of $1-I_+/I(\vec{k})\mathrm{Re}B(\vec{k})$ are shown for $\hbar\omega_+=117$ meV, $\hbar\omega_-=121$ meV (or $\Delta=-6.07\times10^{12}$ sec^{-1}), $\vec{\eta}_+||\vec{\eta}_-||[001]$, and $\vec{k}$ in the [111] direction. The solid curve is for a pump intensity of 1 MW/cm^2, and the dashed curve is for a pump intensity of 10 MW/cm^2. From Fig. 4(a), we see that for small detuning ($\Delta\ll1/T_2$), the factor $1-I_+/I(\vec{k})\mathrm{Re}B(\vec{k})$ is less than unity for all values of $\hbar\Omega(\vec{k})$, and the probe absorption coefficient is reduced as compared to the absorption with only hole-burning effects. As the detuning is increased, the factor $1-I_+/I(\vec{k})\mathrm{Re}B(\vec{k})$ increases and exceeds unity for some values of $\hbar\Omega(\vec{k})$ as shown in Fig. 4(b). For $\Delta=-6.07\times10^{12}$ sec^{-1}, we find that for states with $\hbar\Omega(\vec{k})$ less than about $\hbar\omega_-$, the value of $1-I_+/I(\vec{k})\mathrm{Re}B(\vec{k})$ is greater than one, and for states with $\hbar\Omega(\vec{k})$ greater than about $\hbar\omega_-$, $1-I_+/I(\vec{k})\mathrm{Re}B(\vec{k})$ is less than unity. For a state with $1-I_+/I(\vec{k})\mathrm{Re}B(\vec{k})$ greater than unity, the probe absorption associated with that state in the integration over $\vec{k}$ space is increased as compared with the hole-burning results alone, and for a state with $1-I_+/I(\vec{k})\mathrm{Re}B(\vec{k})$ less than one, the probe absorption associated with that state is decreased as compared with the hole-burning results alone. Thus for $\Delta=-6.07\times10^{12}$ sec^{-1} the net effect of the nonlinear coupling of the two beams on $\alpha_-(\omega_-,I_+)$ is small due to the cancellation in the integration over $\vec{k}$ space in Eq. (16).

By numerically integrating Eq. (16), we calculate the line shape for the absorption coefficient of the probe beam in the presence of a saturating pump laser. We consider the case in which the pump laser is at a fixed wavelength and the probe can be tuned in wavelength in the vicinity of the resonant region of the pump. The probe absorption coefficient is calculated for a pump laser at 10.6 μm (since experimental information[11] exists for this case) and normalized to its value without the presence of the pump laser.

The experiments of Ref. 11 were done at room temperature with a pump laser at $\lambda=10.6\ \mu$m and a sample with a hole concentration of 7.1×10^{15} cm^{-3}. The polarization directions were parallel for the pump and probe waves. The pump and probe beams propagated in approximately opposite directions. The intensity of the pump beam was not determined due to a calibration problem. (See the note added in proof of Ref. 11.) Even if the pump intensity were accurately known, comparison of the absolute magnitude of the reduction in probe absorption by the pump beam is complicated by geometrical effects (radial beam shapes, pump attenuation, extent of beam overlap, etc.). For these reasons, we fix a pump intensity to give the reported magnitude of the absorption reduction at $\Delta=0$ and compare the line shape with the measured results. The calculated results for $\alpha_-(\omega_-,I_+)/\alpha(\omega_-)$ are shown by the solid curves in Fig. 5 for pump intensities of 0.39 and 1.8 MW/cm^2. Also shown by the dashed curves are the calculated results in which only the hole-burning effect is included [i.e., replace ReB with zero in Eq. (16)] for pump intensities of 0.39 and 1.8 MW/cm^2. Having fit the magnitude of the calculated absorption reduction to the magnitude of the measured absorption reduction at $\Delta=0$, we see that the composite line shape of the probe absorption as a function of the detuning of the pump and probe beams is in good agreement with the measured results. Comparing the complete calculation with the calculation including only the hole-burning effect, we see that the coherent coupling between the pump and probe significantly modifies the probe absorption line shape. Compared with the hole-burning-only result, the probe absorption is significantly reduced at small detuning and is slightly increased at large detuning.

When the pump and probe beams are nearly unidirectional (i.e., $\vec{K}_+$ and $\vec{K}_-$ nearly parallel), a new wave is generated at $2\omega_+-\omega_-$ by the current-density component $\vec{R}^{(1)}$. The maximum intensity reached by this generated wave was estimated as a fraction ξ of the incident intensity of the probe beam, where ξ is given by Eq. (17). Values

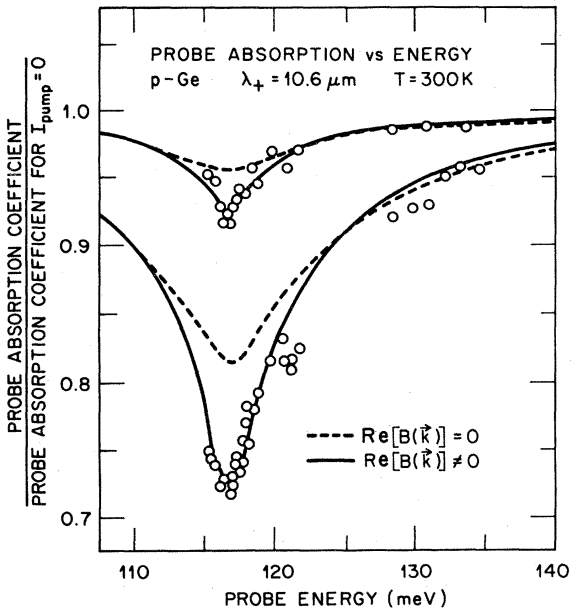

FIG. 5. Values for the absorption coefficient of the probe beam (normalized to the probe absorption coefficient for small pump intensities) as a function of the probe photon energy for a pump photon energy of 117 meV (i.e., $\lambda_+ = 10.6\ \mu m$). The polarization of each beam is taken to be in the [001] direction. The top (bottom) solid curve shows the normalized probe absorption coefficient as calculated from Eq. (16b) for a pump intensity of 0.39 MW/cm^2 (1.8 MW/cm^2). The top (bottom) dashed curve shows the normalized probe absorption coefficient where only the incoherent hole-burning contribution is included [i.e., Re(B) is replaced with zero in Eq. (16b)] for a pump intensity of 0.39 MW/cm^2 (1.9 MW/cm^2). The experimental data of Ref. 11 are shown for comparison by the solid points in the figure.

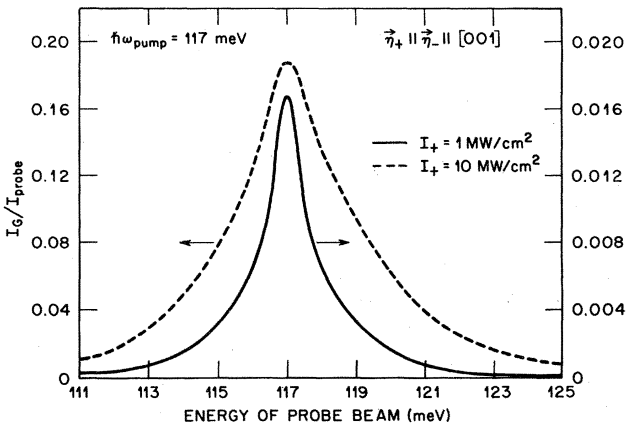

FIG. 6. Approximate values for the intensity of the generated wave at frequency $2\omega_+ - \omega_-$, normalized to the intensity of the probe beam, as a function of the photon energy of the probe. The pump beam is taken to be unidirectional with the probe and having a photon energy of 117 meV. The polarization of both the pump and probe beams are taken to be in the [001] direction. The solid (dashed) line shows values for ξ ($\simeq I_G/I_{probe}$) for a pump intensity of 1 MW/cm^2 (10 MW/cm^2). Values for ξ at $I_+ = 1$ MW/cm^2 are shown to the right in the figure, and the values at $I_+ = 10$ MW/cm^2 are shown to the left.

of ξ are plotted in Fig. 6 as a function of probe frequency for both $\vec{\eta}_+$ and $\vec{\eta}_-$, in the [001] direction, $\theta = 0$, and $\hbar\omega_+ = 117$ meV. The solid line is for a pump intensity of 1 MW/cm^2 (i.e., I_+ somewhat less than I_s) and the dashed line is for a pump intensity of 10 MW/cm^2 (i.e., I_+ somewhat greater than I_s). We find that ξ increases monotonically with increasing I_+ and is strongly dependent on the pump intensity (note the scale change in the figure). We also see that ξ is peaked at $\omega_+ = \omega_-$, and that the curve is more sharply peaked at low pump powers than at high powers. For I_+ greater than I_s and $\hbar\omega_-$ within a few millielectron volts of $\hbar\omega_+$, the intensity of the generated beam can become comparable to that of the probe beam.

IV. SUMMARY AND CONCLUSIONS

We have presented a theory describing the interaction of a high-intensity CO_2 pump laser with a low-intensity probe laser which is tuned in the vicinity of the pump frequency in p-type Ge. The main interaction between the optical beams and the p-type Ge results from intervalence-band transitions between the heavy- and light-hole bands. The pump beam tends to saturate those transitions in resonance with it, that is the difference in distribution functions $f_h^{(0)}(\vec{k}) - f_l^{(0)}(\vec{k})$ is reduced from the equilibrium value for states with wave vector $\vec{k}$ near resonance. Because of the nonlinear interaction between the pump and probe beams, a component in the population difference $f_h^{(1)}(\vec{k}) - f_l^{(1)}(\vec{k})$, which oscillates at $(\omega_+ - \omega_-)t - (\vec{K}_+ - \vec{K}_-)\cdot\vec{r}$, is generated. This oscillating component can be viewed as a spatial and temporal grating which mixes the pump and probe beams. The pump and probe beams induce three components in the current density by the intervalence-band transitions: $\vec{R}^{(0)}$ which oscillates at $\omega_+ t - \vec{K}_+\cdot\vec{r}$, $\vec{I}^{(1)}$ which oscillates at $\omega_- t - \vec{K}_-\cdot\vec{r}$, and $\vec{R}^{(1)}$ which oscillates at $(2\omega_+ - \omega_-)t - (2\vec{K}_+ - \vec{K}_-)\cdot\vec{r}$. The current-density component $\vec{R}^{(0)}$ leads to absorption of the pump beam and is independent of the probe. The current-density component $\vec{I}^{(1)}$ leads to absorption of the probe beam. It is influenced by the pump beam in two ways: Absorption of the probe is reduced by the pump saturation of the population difference $[f_h^{(0)}(\vec{k}) - f_l^{(0)}(\vec{k})]$ in the resonant region (hole-burning effect), and there exists an oscillating component of the population difference, which leads to an energy transfer between the two beams. This coupling of the beams reduces the probe absorption when the pump and probe frequencies are close and increases slightly the probe absorption when there is a larger difference between the frequencies of the two beams. The current-density component $\vec{R}^{(1)}$ leads to the generation of a third optical beam at $(2\omega_+ - \omega_-)t - (2\vec{K}_+ - \vec{K}_-)\cdot\vec{r}$. For conditions in which $\vec{K}_+$ and $\vec{K}_-$ are nearly parallel, the pump intensity is greater than I_s, and the pump and probe frequencies are nearly equal, the intensity of this

generated wave can become comparable to that of the probe beam. We have presented detailed calculations for the oscillating population component $[f_h^{(1)}(\vec{k})-f_l^{(1)}(\vec{k})]$, the current-density components, the absorption of the probe beam as a function of probe frequency, and the intensity of the generated beam as a function of probe frequency. We have compared our calculated results for the probe absorption line shape with the measured results of Ref. 11 and found good agreement.

ACKNOWLEDGMENTS

The authors thank L. S. Darken and J. T. Luck for assistance with the preparation of this manuscript and R. F. Wood for his encouragement and many useful comments. This work was partly supported by the Division of Materials Sciences, U.S. Department of Energy, under Contract No. W-7405-eng-26 with Union Carbide Corporation. The work of R. B. James was also partly supported by the Oak Ridge National Laboratory through the Eugene P. Wigner Fellowship Fund. The work of D. L. Smith was partly supported by the Office of Naval Research under Contract No. N00014-81-K-0305.

APPENDIX A: EFFECT OF THE INDUCED CURRENT DENSITY ON THE OPTICAL BEAM PROPAGATION

In this appendix we discuss the effect of the induced current density, calculated to first order in the probe-field strength, on the propagation of the optical beams. The propagation of the optical beams is described by the wave equation

$$\nabla^2\vec{A}-\frac{\epsilon}{c^2}\frac{\partial^2\vec{A}}{\partial t^2}=-\frac{4\pi}{c}\vec{J}\ , \tag{A1}$$

where $\vec{J}$ is the induced current density owing to intervalence-band transitions. To first order in the probe-field strength, $\vec{J}$ is given by

$$\begin{aligned}\vec{J}=&(\bar{\vec{R}}^{(0)}e^{i(\omega_+t-\vec{K}_+\cdot\vec{r})}+\text{c.c.})\\&+(\bar{\vec{R}}^{(1)}e^{i[(2\omega_+-\omega_-)t-(2\vec{K}_+-\vec{K}_-)\cdot\vec{r}]}+\text{c.c.})\\&+(\bar{\vec{I}}^{(1)}e^{i(\omega_-t-\vec{K}_-\cdot\vec{r})}+\text{c.c.})\ ,\end{aligned} \tag{A2}$$

where $\bar{\vec{R}}^{(0)}=\sum_{\vec{k}}\vec{R}^{(0)}(\vec{k})$, $\bar{\vec{R}}^{(1)}=\sum_{\vec{k}}\vec{R}^{(1)}(\vec{k})$, and $\bar{\vec{I}}^{(1)}=\sum_{\vec{k}}\vec{I}^{(1)}(\vec{k})$. Here, $\vec{R}^{(0)}(\vec{k})$ is given by Eq. (7), $\vec{R}^{(1)}(\vec{k})$ by Eq. (13), and $\vec{I}^{(1)}(\vec{k})$ by Eq. (14). From the form of $\vec{J}$, it is clear that $\vec{A}$ will take the form[27]

$$\begin{aligned}\vec{A}=&\frac{A_+(z_+)}{2}\vec{\eta}_+(e^{i(\omega_+t-K_+z_+)}+\text{c.c.})\\&+\frac{A_-(z_-)}{2}\vec{\eta}_-(e^{i(\omega_-t-K_-z_-)}+\text{c.c})\\&+\left[\frac{G(z)}{2}\vec{\eta}e^{i[(2\omega_+-\omega_-)t-|2\vec{K}_+-\vec{K}_-|z]}+\text{c.c.}\right],\end{aligned} \tag{A3}$$

where $z_\pm$ is in the direction $\vec{K}_\pm$ and z is in the direction of $2\vec{K}_+-\vec{K}_-$. We assume that the amplitude functions $A_+(z_+)$, etc., are slowly varying so that we need keep only their first (and not second) spatial derivatives. By substituting Eqs. (A2) and (A3) into the wave equation, equating coefficients of terms with the same temporal dependence and taking the dot product with the polarization vectors, one obtains the equations

$$A_+(K_+)^2+2iK_+\frac{\partial A_+}{\partial z_+}-\frac{\epsilon}{c^2}\omega_+^2A_+=\frac{8\pi}{c}\bar{\vec{R}}^{(0)}\cdot\vec{\eta}_+\ , \tag{A4a}$$

$$A_-(K_-)^2+2iK_-\frac{\partial A_-}{\partial z_-}-\frac{\epsilon}{c^2}\omega_-^2A_-=\frac{8\pi}{c}\vec{I}^{(1)}\cdot\vec{\eta}_-\ , \tag{A4b}$$

and

$$G|2\vec{K}_+-\vec{K}_-|^2+2i|2\vec{K}_+-\vec{K}_-|\frac{\partial G}{\partial z}-\frac{\epsilon}{c^2}(2\omega_+-\omega_-)^2G=\frac{8\pi}{c}\bar{\vec{R}}^{(1)}\cdot\vec{\eta}\ . \tag{A4c}$$

[Note: In general, the current-density components (e.g., $\vec{I}^{(1)}$) are not necessarily parallel to the corresponding polarization vector (i.e., $\vec{\eta}_-$). This implies that the polarization vectors are functions of position as the beam propagates through the medium. One could describe this effect by allowing the polarization to rotate and dotting the wave equation with a unit vector orthogonal to the polarization vector.] From the real and imaginary parts of Eq. (A4a), one finds $|\vec{K}_+|$ from which one obtains the absorption coefficient of the pump beam α_+.[13] From the real and imaginary parts of Eq. (A4b), one finds

$$|K_-|^2=\frac{\epsilon}{c^2}\omega_-^2+\frac{8\pi}{c}\frac{\text{Re}(\bar{\vec{I}}^{(1)}\cdot\vec{\eta}_-)}{A_-} \tag{A5a}$$

and

$$\frac{1}{A_-}\frac{\partial A_-}{\partial z_-}=\frac{4\pi\,\text{Im}(\bar{\vec{I}}^{(1)}\cdot\vec{\eta}_-)}{cK_-A_-}\ . \tag{A5b}$$

Equation (16) for the probe absorption coefficient follows from Eq. (A5b).

We next consider the wave at frequency $2\omega_+-\omega_-$, which is generated by the current-density term $\vec{R}^{(1)}$ and described by the field amplitude $G(z)$. We first notice that in the derivation of the current-density expression this wave was not considered. (Notice, for example, there is no term in the current density that describes absorption of this wave.) For a self-consistent description of this wave, it is necessary to rederive a current-density expression allowing for the presence of this generated wave in addition to the pump and probe waves. Such a procedure is quite tractable within our basic approach. Here, however, we will use the previous expressions for the current density (correct for small G) to determine conditions under which this wave can be generated and to approximately estimate the intensities it can reach.

Equation (A4c), which describes the generation of this wave at $2\omega_+-\omega_-$, can be written as

$$\frac{\partial G(z)}{\partial z}-\rho G(z)=\gamma(z)\ , \tag{A6a}$$

where

$$\rho=\frac{(\epsilon/c^2)(2\omega_+-\omega_-)^2-|2\vec{K}_+-\vec{K}_-|^2}{2i\,|2\vec{K}_+-\vec{K}_-|} \tag{A6b}$$

and

$$\gamma(z)=\frac{8\pi}{c}\frac{\bar{\vec{R}}^{(1)}(z)\cdot\vec{\eta}}{2i\,|2\vec{K}_+-\vec{K}_-|}\ . \tag{A6c}$$

Here $\vec{\eta}$ is in the direction of $\bar{\vec{R}}^{(1)}$. $\bar{\vec{R}}^{(1)}(z)$ is a function of z through the z dependence of the pump and probe intensities. (Actually, there is also a small z dependence of ρ because of the intensity dependences of $\vec{K}_+$ and $\vec{K}_-$.[13,28] This should be included for precise calculation, but for our purpose here, we neglect it.) We also take the z dependence of $\bar{\vec{R}}^{(1)}(z)$ as externally fixed (i.e., the position dependence of the pump and probe intensities are specified). For a self-consistent description, the intensities of the probe and generated beams would have to be calculated simultaneously if the conditions were such that $|G(z)|$ becomes comparable to $|A_-(z)|$.

As a boundary condition, we set $G(0)=0$ (i.e., the plane $z=0$ is the Ge surface on which the pump and probe lasers are incident). The solution of Eq. (A6a) is then

$$G(z)=e^{\rho z}\int_0^z e^{-\rho z'}\gamma(z')dz'\ . \tag{A7}$$

We write

$$|K_\pm|^2=\frac{\epsilon}{c^2}\omega_\pm+\delta_\pm\ , \tag{A8}$$

where δ_- is given by Eq. (A5a) and δ_+ is found in the same way from Eq. (A4a). Taking $\delta_\pm$ to be small quantities and $\omega_+\simeq\omega_-=\omega$ and expanding ρ to first order in small quantities, one finds

$$\rho\simeq i\left[\frac{8\pi}{\sqrt{\epsilon}\omega}\frac{\mathrm{Re}(\bar{\vec{R}}^{(0)}\cdot\vec{\eta}_+)}{A_+}(2-\cos\theta)-\frac{4\pi}{\sqrt{\epsilon}\omega}\frac{\mathrm{Re}(\bar{\vec{I}}^{(1)}\cdot\vec{\eta}_-)}{A_-}(2\cos\theta-1)+\frac{\frac{2\sqrt{\epsilon}}{c}\omega(1-\cos\theta)}{\sqrt{5-4\cos\theta}}\right]\ , \tag{A9}$$

where θ is the angle between $\vec{K}_+$ and $\vec{K}_-$. By comparing Eqs. (A9) and (A7), it is clear that unless $\cos\theta\simeq1$, ρ will be of the order of $1/\lambda$ and the integral will oscillate rapidly. Thus we only consider this case and write

$$\rho\simeq i\left[\frac{8\pi}{\sqrt{\epsilon}\omega}\frac{\mathrm{Re}(\bar{\vec{R}}^{(0)}\cdot\vec{\eta}_+)}{A_+}-\frac{4\pi}{\sqrt{\epsilon}\omega}\frac{\mathrm{Re}[\bar{\vec{I}}^{(0)}\cdot\vec{\eta}_-]}{A_-}+\frac{2\sqrt{\epsilon}}{c}\omega(1-\cos\theta)\right]\ , \tag{A10}$$

where $(\sqrt{\epsilon}\omega)/c$ is assumed to be much larger than the first two terms in the brackets.

In order to evaluate the integral in Eq. (A7), we must know the position dependence of $\gamma(z)$. This could be determined precisely by integrating Eq. (A5c) and the corresponding equation for $I_+(z)$. Here, however, we simply note that $\gamma(z)$ is proportional to $I_+(z)$ and $A_-(z)$, and we use the simple approximate form

$$\gamma(z)\simeq\gamma(0)e^{-(\alpha_++\alpha_-/2)z}\ , \tag{A11}$$

and take α_+ and α_- as position independent. (Since $\cos\theta\simeq1$, we have $z_+\simeq z_-\simeq z$.) With these approximations, Eq. (A7) is integrated and the results squared to give the following expression for the intensity of the generated beam:

$$I_G(z)=I_-(0)\,|1-e^{-(\rho+\alpha_++\alpha_-/2)z}|^2\left|\frac{(\bar{\vec{R}}^{(1)}\cdot\vec{\eta}/A_-)}{\frac{2(\bar{\vec{R}}^{(0)}\cdot\vec{\eta}_+)}{A_+}-\left[\frac{\bar{\vec{I}}^{(1)}\cdot\vec{\eta}_-}{A_-}\right]^*+\frac{\epsilon\omega^2}{2\pi c}(1-\cos\theta)}\right|^2\ , \tag{A12}$$

where I_G is the intensity of the generated wave at $2\omega_+-\omega_-$ and $I_-(0)$ is the incident intensity of the probe beam. Because of the various approximations which were made in its derivation, Eq. (A12) is very rough. But it does suggest that the second squared quantity can give an approximate estimate of the intensity which the generated wave can reach.

APPENDIX B: HIGHER-ORDER TERMS IN THE PERTURBATION SERIES

In this appendix we derive higher-order equations in the perturbation by the probe-field strength. In general, the nth order ($n\geq1$) equation for the current density owing to the intervalence-band transitions is given by

$$\frac{d^2}{dt^2}\vec{J}^{(n)}(\vec{k})+\frac{2}{T_2(\vec{k})}\frac{d}{dt}\vec{J}^{(n)}(\vec{k})+\Omega^2(\vec{k})\vec{J}^{(n)}(\vec{k})$$
$$=\frac{N_h e^2}{\hbar^2 m^2 c}\sum_{\substack{b\in h\\ c\in l}}\left[\left\{[f_h^{(n-1)}(\vec{k})-f_l^{(n-1)}(\vec{k})]\hbar\Omega(\vec{k})[\vec{\eta}_-\cdot\vec{P}_{bc}(\vec{k})\vec{P}_{cb}(\vec{k})+\vec{\eta}_-\cdot\vec{P}_{cb}(\vec{k})\vec{P}_{bc}(\vec{k})]\frac{A_-}{2}(e^{i(\omega_- t-\vec{K}_-\cdot\vec{r})}+\text{c.c.})\right\}\right.$$
$$\left.+\left\{[f_h^{(n)}(\vec{k})-f_l^{(n)}(\vec{k})]\hbar\Omega(\vec{k})[\vec{\eta}_+\cdot\vec{P}_{bc}(\vec{k})\vec{P}_{cb}(\vec{k})+\vec{\eta}_+\cdot\vec{P}_{cb}(\vec{k})\vec{P}_{bc}(\vec{k})]\frac{A_+}{2}(e^{i(\omega_+ t-\vec{K}_+\cdot\vec{r})}+\text{c.c.})\right\}\right], \tag{B1}$$

where $\vec{J}^{(n)}(\vec{k})$, $f_h^{(n)}(\vec{k})$, and $f_l^{(n)}(\vec{k})$ are defined by Eq. (5). In a similar way, we write general expressions to calculate $f_h^{(n)}(\vec{k})$ and $f_l^{(n)}(\vec{k})$ as follows:

$$\frac{df_h^{(n)}(\vec{k})}{dt}=-\frac{1}{2N_h c\hbar\Omega(\vec{k})}\left[\left\{\left[\frac{d}{dt}\vec{J}^{(n-1)}(\vec{k})\right]\cdot\vec{\eta}_-\frac{A_-}{2}(e^{i(\omega_- t-\vec{K}_-\cdot\vec{r})}+\text{c.c})\right.\right.$$
$$\left.\left.+\left[\frac{d}{dt}\vec{J}^{(n)}(\vec{k})\right]\cdot\vec{\eta}_+\frac{A_+}{2}(e^{i(\omega_+ t-\vec{K}_+\cdot\vec{r})}+\text{c.c.})\right\}\right]$$
$$-\sum_{c,\vec{k}'}[R_{h,\vec{k}\to c,\vec{k}'}f_h^{(n)}(\vec{k})-R_{c,\vec{k}'\to h,\vec{k}}f_c^{(n)}(\vec{k}')] \tag{B2}$$

and

$$\frac{df_l^{(n)}(\vec{k})}{dt}=\frac{1}{2N_h c\hbar\Omega(\vec{k})}\left[\left\{\left[\frac{d}{dt}\vec{J}^{(n-1)}(\vec{k})\right]\cdot\vec{\eta}_-\frac{A_-}{2}(e^{i(\omega_- t-\vec{K}_-\cdot\vec{r})}+\text{c.c.})\right.\right.$$
$$\left.\left.+\left[\frac{d}{dt}\vec{J}^{(n)}(\vec{k})\right]\cdot\vec{\eta}_+\frac{A_+}{2}(e^{i(\omega_+ t-\vec{K}_+\cdot\vec{r})}+\text{c.c.})\right\}\right]$$
$$-\sum_{c,\vec{k}'}[R_{l,\vec{k}\to c,\vec{k}'}f_l^{(n)}(\vec{k})-R_{c,\vec{k}'\to l,\vec{k}}f_c^{(n)}(\vec{k}')]\,. \tag{B3}$$

For low-intensity probe beams ($I_- \ll I_s$), the perturbation series can be truncated at first order in the probe-field strength. The first-order expressions for $\vec{J}^{(1)}(\vec{k})$ and $F_h^{(1)}(\vec{k})-F_l^{(1)}(\vec{k})$ are explicitly written earlier in the manuscript. The second-order results can be written using Eqs. (B1)—(B3). From the equations it is clear that $F_h^{(2)}(\vec{k})-F_l^{(2)}(\vec{k})$ has steady-state terms and terms which oscillate at $\pm i[2(\omega_+-\omega_-)t-2(\vec{K}_+-\vec{K}_-)\cdot\vec{r}]$. The second-order term in the current density $\vec{J}^{(2)}(\vec{k})$ has terms which oscillate at $\omega_+ t-\vec{K}_+\cdot\vec{r}$ and $[\omega_+\pm 2(\omega_+-\omega_-)]t-[\vec{K}_+\pm 2(\vec{K}_+-\vec{K}_-)]\cdot\vec{r}$. The dc terms in $f_h^{(2)}(\vec{k})$ and $f_l^{(2)}(\vec{k})$, the terms in $f_h^{(1)}(\vec{k})-f_l^{(1)}(\vec{k})$ which oscillate at $\pm[(\omega_+-\omega_-)t-(\vec{K}_+-\vec{K}_-)\cdot\vec{r}]$ and the terms in $\vec{J}^{(2)}(\vec{k})$ which oscillate at $\omega_+ t-\vec{K}_+\cdot\vec{r}$ all couple in Eqs. (B1)—(B3). The coupled equations can be solved for the steady-state component in $f_h^{(2)}(\vec{k})-f_l^{(2)}(\vec{k})$, which is second-order in the probe-field strength. We then write

$$f_h^{(2)}(\vec{k})=F_h^{(2)}(\vec{k},0)+[F_h^{(2)}(\vec{k},2\Delta)e^{i[2(\omega_+-\omega_-)t-2(\vec{K}_+-\vec{K}_-)\cdot\vec{r}]}+\text{c.c.}]\,, \tag{B4}$$

$$f_l^{(2)}(\vec{k})=F_l^{(2)}(\vec{k},0)+[F_l^{(2)}(\vec{k},2\Delta)e^{i[2(\omega_+-\omega_-)t-2(\vec{K}_+-\vec{K}_-)\cdot\vec{r}]}+\text{c.c.}]\,, \tag{B5}$$

and

$$\vec{J}^{(2)}(\vec{k})=[\vec{J}^{(2)}(\vec{k},\omega_+)e^{i[\omega_+ t-\vec{K}_+\cdot\vec{r}]}+\text{c.c.}]+[\vec{J}^{(2)}(\vec{k},\omega_++2\Delta)e^{i[(3\omega_+-2\omega_-)t-(3\vec{K}_+-2\vec{K}_-)\cdot\vec{r}}+\text{c.c.}]$$
$$+[\vec{J}^{(2)}(\vec{k},\omega_+-2\Delta)e^{i[(-\omega_++2\omega_-)t-(-\vec{K}_++2\vec{K}_-)\cdot\vec{r}]}+\text{c.c.}]\,. \tag{B6}$$

The calculated dc values for $F_h^{(2)}(\vec{k},0)-F_l^{(2)}(\vec{k},0)$ give the effect of the probe intensity on the state filling of the resonant transition. This term slightly modifies the optical excitation rate between states in the resonant region of the heavy-hole band, and thus produces a small change in the rate of energy absorption of the pump beam. The terms $\vec{J}^{(2)}(\omega_+ \pm 2\Delta)$ produce new waves at the sidebands $(\omega_+ \pm 2\Delta)$. As one goes to higher orders in the probe-field strength ($n \geq 3$), new waves are generated at still higher-order sidebands, and population of free holes in the resonant region has terms which oscillate at higher-order harmonics of the beat frequency. However, these higher-order terms are much smaller than the terms which are first order in the probe-field strength for probe intensities I_- much less than the saturation intensity of the resonant intervalence-band transition.

---

*Permanent address: Honeywell Systems and Research Center, Minneapolis, MN 55440.

[1]A. H. Kahn, Phys. Rev. 97, 1647 (1955).
[2]C. R. Phipps, Jr., and S. J. Thomas, Opt. Lett. 1, 93 (1977).
[3]R. L. Carlson, M. D. Montgomery, J. S. Ladish, and C. M. Lockhart, IEEE J. Quantum Electron. QE-13 35D (1977).
[4]F. Keilmann, IEEE J. Quantum Electron. QE-12 592 (1976).
[5]C. R. Phipps, S. J. Thomas, J. Ladish, S. J. Czuchlewski, and J. F. Figueria, IEEE J. Quantum Electron. QE-13 36D (1977).
[6]R. B. James, E. Schweig, D. L. Smith, and T. C. McGill, Appl. Phys. Lett. 40, 231 (1982).
[7]R. B. James and D. L. Smith, Phys. Rev. Lett. 42, 1495 (1979).
[8]M. Kawai and T. Miyakawa, Jpn. J. Appl. Phys. 20, 369 (1981).
[9]M. Sargent III, Opt. Commun. 20, 298 (1977).
[10]M. Kawai and T. Miyakawa, IEEE J. Quantum Electron. QE-17 1996 (1981).
[11]F. Keilmann, Appl. Phys. 14, 29 (1977).
[12]P. J. Bishop, A. F. Gibson, and M. F. Kimmitt, J. Phys. D 9, L101 (1976).
[13]R. B. James and D. L. Smith, Phys. Rev. B 21, 3502 (1980).
[14]E. V. Baklanov and V. P. Chebotaev, Zh. Eksp. Teor. Fiz. 61, 922 (1971) [Sov. Phys.—JETP 33, 300 (1971)].
[15]S. Haroche and F. Hartmann, Phys. Rev. A 6, 1280 (1972).
[16]M. Sargent III, Appl. Phys. 9, 127 (1976).
[17]M. Sargent III and P. E. Toschek, Appl. Phys. 11, 107 (1976).
[18]M. Sargent III, P. E. Toschek, and H. G. Danielmeyer, Appl. Phys. 11, 55 (1976).
[19]W. Kaiser, R. J. Collins, and H. Y. Fan, Phys. Rev. 91, 1380 (1953).
[20]A. J. Bishop and A. F. Gibson, Appl. Opt. 12, 2549 (1973).
[21]R. B. James and D. L. Smith, IEEE J. Quantum Electron. QE-18, 1841 (1982).
[22]E. O. Kane, J. Phys. Chem. Solids 1, 82 (1956).
[23]J. C. Hensel and K. Suzuki, Phys. Rev. B 9, 4219 (1974).
[24]D. M. Brown and R. Bray, Phys. Rev. 127, 1593 (1962).
[25]R. B. James and D. L. Smith, J. Appl. Phys. 51, 2836 (1980).
[26]R. B. James and D. L. Smith, Solid State Commun. 33, 395 (1980).
[27]Equation (A3) assumes a particular phase relation between the pump and probe beams. However, none of the results of the paper depend on this phase relation.
[28]R. B. James and D. L. Smith, Phys. Rev. B 23, 4044 (1981).